REPORT DOCUMENTATION PAGE

Form Approved OMB NO. 0704-0188

The public reporting burden for this collection of information is estimated to average 1 hour per response, including the time for reviewing instructions, searching existing data sources, gathering and maintaining the data needed, and completing and reviewing the collection of information. Send comments regarding this burden estimate or any other aspect of this collection of information, including suggesstions for reducing this burden, to Washington Headquarters Services, Directorate for Information Operations and Reports, 1215 Jefferson Davis Highway, Suite 1204, Arlington VA, 22202-4302. Respondents should be aware that notwithstanding any other provision of law, no person shall be subject to any oenalty for failing to comply with a collection of information if it does not display a currently valid OMB control number.
PLEASE DO NOT RETURN YOUR FORM TO THE ABOVE ADDRESS.

1. REPORT DATE (DD-MM-YYYY)	2. REPORT TYPE	3. DATES COVERED (From - To)
03-01-2011	Final Report	1-Jul-2009 - 30-Jun-2010

4. TITLE AND SUBTITLE	5a. CONTRACT NUMBER
Equation of state of ballistic gelatin (II)	W911NF-09-1-0297
	5b. GRANT NUMBER
	5c. PROGRAM ELEMENT NUMBER
	611102

6. AUTHORS	5d. PROJECT NUMBER
Muhetaer Aihaiti, Russell J. Hemley	5e. TASK NUMBER
	5f. WORK UNIT NUMBER

7. PERFORMING ORGANIZATION NAMES AND ADDRESSES	8. PERFORMING ORGANIZATION REPORT NUMBER
Carnegie Institution of Washington Carnegie Institution of Washington 1530 P ST NW Washington, DC 20005 -1910	

9. SPONSORING/MONITORING AGENCY NAME(S) AND ADDRESS(ES)	10. SPONSOR/MONITOR'S ACRONYM(S)
U.S. Army Research Office P.O. Box 12211 Research Triangle Park, NC 27709-2211	ARO
	11. SPONSOR/MONITOR'S REPORT NUMBER(S)
	55048-EG.1

12. DISTRIBUTION AVAILIBILITY STATEMENT

Approved for Public Release; Distribution Unlimited

13. SUPPLEMENTARY NOTES

The views, opinions and/or findings contained in this report are those of the author(s) and should not contrued as an official Department of the Army position, policy or decision, unless so designated by other documentation.

14. ABSTRACT

We determined the equation of state of ballistic gelatin (20%) using Brillouin scattering spectroscopy with diamond anvil cells by measuring the pressure dependence of the sound velocities of the material from ambient pressure to 12 GPa at room temperature. We extended these measurements to 4%- and 10% gelatin solutions up to 12 GPa. Consistent results for 4%- and 10%-gelatin in several experimental runs were not obtained. For comparison purposes, we also measured the pressure dependence of sound velocity of lamb tissues up to 10 GPa. We analyzed

15. SUBJECT TERMS

gelatin solutions, equation of state, Brillouin scattering, high pressure

16. SECURITY CLASSIFICATION OF:			17. LIMITATION OF ABSTRACT	15. NUMBER OF PAGES	19a. NAME OF RESPONSIBLE PERSON
a. REPORT	b. ABSTRACT	c. THIS PAGE			Russell Hemley
UU	UU	UU	UU		19b. TELEPHONE NUMBER
					202-478-8951

Standard Form 298 (Rev 8/98)
Prescribed by ANSI Std. Z39.18

Report Title

Equation of state of ballistic gelatin (II)

ABSTRACT

We determined the equation of state of ballistic gelatin (20%) using Brillouin scattering spectroscopy with diamond anvil cells by measuring the pressure dependence of the sound velocities of the material from ambient pressure to 12 GPa at room temperature. We extended these measurements to 4%- and 10% gelatin solutions up to 12 GPa. Consistent results for 4%- and 10%-gelatin in several experimental runs were not obtained. For comparison purposes, we also measured the pressure dependence of sound velocity of lamb tissues up to 10 GPa. We analyzed the Brillouin data using the Vinet equation of state and obtained the bulk modulus and its pressure derivative. We compared the parameters obtained for gelatin with several relevant polymer materials as well as water. In addition, we discussed the possibility of ultrasonic measurements on gelatin solutions under similar conditions. Such measurements are expected to provide useful information in understanding of the relaxation phenomena in gelatins.

List of papers submitted or published that acknowledge ARO support during this reporting period. List the papers, including journal references, in the following categories:

(a) Papers published in peer-reviewed journals (N/A for none)

Number of Papers published in peer-reviewed journals: 0.00

(b) Papers published in non-peer-reviewed journals or in conference proceedings (N/A for none)

Aihaiti, M.; Hemley, R. J. Equation of State of Ballistic Gelatin; 50533-EG.1; Army Research Office Report; Carnegie Institution of Washington, 2008.

Number of Papers published in non peer-reviewed journals: 1.00

(c) Presentations

1. Army Research Laboratory Fellows Symposium;
Presenter: Russell J. Hemley
Title: New finding and phenomena in materials under extreme conditions
Date: October 6th, 2010

2. Army Research Laboratory, invited talk
Presenter: Muhetaer Aihaiti
Title: Spectroscopic studies of polymers, gelatins and AlON
Date: October 21st, 2010

Number of Presentations: 2.00

Non Peer-Reviewed Conference Proceeding publications (other than abstracts):

Number of Non Peer-Reviewed Conference Proceeding publications (other than abstracts):   0

Peer-Reviewed Conference Proceeding publications (other than abstracts):

Number of Peer-Reviewed Conference Proceeding publications (other than abstracts):   0

(d) Manuscripts

Number of Manuscripts: 0.00

Patents Submitted

Patents Awarded

Awards

Graduate Students

NAME	PERCENT_SUPPORTED
FTE Equivalent:	
Total Number:	

Names of Post Doctorates

NAME	PERCENT_SUPPORTED
FTE Equivalent:	
Total Number:	

Names of Faculty Supported

NAME	PERCENT_SUPPORTED
FTE Equivalent:	
Total Number:	

Names of Under Graduate students supported

NAME	PERCENT_SUPPORTED
FTE Equivalent:	
Total Number:	

Student Metrics

This section only applies to graduating undergraduates supported by this agreement in this reporting period

The number of undergraduates funded by this agreement who graduated during this period: 0.00

The number of undergraduates funded by this agreement who graduated during this period with a degree in science, mathematics, engineering, or technology fields: 0.00

The number of undergraduates funded by your agreement who graduated during this period and will continue to pursue a graduate or Ph.D. degree in science, mathematics, engineering, or technology fields: 0.00

Number of graduating undergraduates who achieved a 3.5 GPA to 4.0 (4.0 max scale): 0.00

Number of graduating undergraduates funded by a DoD funded Center of Excellence grant for Education, Research and Engineering: 0.00

The number of undergraduates funded by your agreement who graduated during this period and intend to work for the Department of Defense 0.00

The number of undergraduates funded by your agreement who graduated during this period and will receive scholarships or fellowships for further studies in science, mathematics, engineering or technology fields: 0.00

Names of Personnel receiving masters degrees

NAME

Total Number:

Names of personnel receiving PHDs

NAME

Total Number:

Names of other research staff

NAME	PERCENT_SUPPORTED	
Muhetaer Aihaiti	1.00	No
FTE Equivalent:	**1.00**	
Total Number:	**1**	

Sub Contractors (DD882)

Inventions (DD882)

Equation of state of ballistic gelatin (II)

Muhetaer Aihaiti (Muhtar Ahart) and Russell J. Hemley

Geophysical Laboratory, Carnegie Institution of Washington
5251 Broad Brach Rd., NW Washington DC 20015

Table of Contents

I. Summary

We determined the equation of state of ballistic gelatin (20%) using Brillouin scattering spectroscopy with diamond anvil cells by measuring the pressure dependence of the sound velocities of the material from ambient pressure to 12 GPa at room temperature. We extended these measurements to 4%- and 10% gelatin solutions up to 12 GPa. Consistent results for 4%- and 10%-gelatin in several experimental runs were not obtained. For comparison purposes, we also measured the pressure dependence of sound velocity of lamb tissues up to 10 GPa. We analyzed the Brillouin data using the Vinet equation of state and obtained the bulk modulus and its pressure derivative. We compared the parameters obtained for gelatin with several relevant polymer materials as well as water. In addition, we discussed the possibility of ultrasonic measurements on gelatin solutions under similar conditions. Such measurements are expected to provide useful information in understanding of the relaxation phenomena in gelatins.

II. Introduction

Polymer-like materials are critically important in science and society, given the diversity of applications of these materials from optics and electronics to garden hoses and soda bottles. Fundamental studies of these materials under variety conditions are central to the field of polymer physics and chemistry. While the chemistry of polymeric chain formation is primarily dictated by the reactivity of the monomer units, the resultant physical properties of a given polymer are highly reliant on network topology and presence or absence of filler materials. External stimuli, temperatures and pressure, have pronounced influence on their mechanical behavior. Many biomaterials are polymers. Gelatin, including its water solution, is extracted by acid or base hydrolysis from collagen, the main matrix material of animal skin, bone, and connective tissue. Gelatin is a collection of large protein molecules similar to amino acid composition. In a given gelatin sample, the molecular weight ranges between 17,000 and 300,000 Daltons. Thus the average molecular weight is used in characterization of the gelatin. One important use for gelatin is as the "model" of human tissue in bullet penetration experiments (Ref. 1). This material is known as "ballistic gelatin." We have reported the equation of state (EOS) for ballistic gelatin (20%) and its elastic behavior in the pressure range of ambient and 12 GPa and the temperature range of 0 to 100 ℃ in Ref. 2.

For comparison purposes, the EOS and mechanical properties of 10%- and 4%-gelatin (water solutions) have been determined from ambient pressure to approximately 12 GPa using a diamond-anvil cell (DAC) in conjunction with Brillouin scattering. We also revisited the 20%-gelatin solution. Considering the fact that gelatin solutions are used here as model systems, in order to make a more direct comparison for military

applications, we measured the pressure dependencies of the sound velocities of several animal tissues including lamb red meat and brain tissues. The work presented here supplies a necessary extension to the current EOS data available for gelatin (Ref. 2). In-situ sound velocities are directly related to elastic parameters, sound velocity measurements can provide useful insight into the microscopic structure of a material.

III. Experimental details

(1) Brillouin scattering experiments

The samples of gelatin (20%, 10%, and 4%) were prepared with the methods described in Ref. 1. Gelatin samples are loaded into a DAC (Fig. 1) with no pressure medium added. Pre-indented (12 GPa) stainless gaskets with a gasket hole of about 120 microns were used. We used a standard ruby fluorescence method to determine the pressure.

We measured the pressure dependencies of velocities of the various samples including 20%-, 10%-, 4%-gelatin, and animal tissues. The detailed description of our Brillouin scattering system, the principle of Brillouin scattering, and diamond anvil cells could be found in Refs. 2-8. Light from a single mode Ar-ion laser (λ=514.5 nm) was used as the excitation source with the average power less than 100 mW. The scattered light was analyzed by a 3+3 tandem Fabry-Perot interferometer, detected by a photon counting photomultiplier, and was outputted to a multichannel scalar. Spectra were taken at each pressure point, and collected for 5 to 60 minutes.

Figure 1 exhibits the symmetric scattering geometry employed in these experiments, the scattering angle was 70°. Since samples were placed symmetrically with respect to the incoming and collected light, and for this particular geometry the frequency

shift of the incident light is independent of the refractive index of the samples, the Brillouin shift can be reduced to

$$\Delta \nu = (2\upsilon / \lambda)\sin(\theta / 2), \qquad (1)$$

where υ is sound velocity, λ=514.5 nm (laser wavelength), and θ=70° is the scattering angle.

(2) Ultrasonic system

The technique of ultrasonic interferometry measurements are widely used in scientific research and industry applications. The same technique has been adopted for use in the diamond anvil cell (Refs. 9 and 10). Briefly, ultrasonic signals from a 1.5 mm thin ZnO transducer are introduced to the sample by means of a glass rod which is pressed against the table face of the diamond anvil carrying the sample (Fig. 2a). Simple principle, a single pulse of ultrasonic signal traveling from the transducer down the buffer rod, through the diamond anvil, and through the sample produces a series of reflections created at each of the interfaces that the signal passes through, we indicated those interfaces as surface 1, 2 and 3 in Fig. 2a. These travel back to the transducer and are recorded as a function of elapsed time.

Practically speaking, as shown in Fig. 2b, two closely spaced pulses P and P' will be used as the input signal, their reflections indicated as 1, 1'; 2, 2'; and 3, 3' at each interface, respectively. These two input pulses can be carefully timed so that the reflection of the first pulse from the far surface of the sample (echo 3) is superimposed on the reflection of the second pulse (echo 2') from the near surface of the sample. The interference of these two signals as they return to the transducer provides a sensitive means for determining the travel time of the signal through the sample.

This interferometric technique eliminates the necessity of measuring the travel times through the buffer rod and diamond, but it is critically dependent upon good energy transfer between the buffer rod and the diamond and between the diamond and the samples. Each maximum and each minimum in the interference pattern results from constructive and destructive interference, respectively, and thus represents a separate measurement of the travel time, t. Thus if sample thickness is known, the velocity can be calculated.

The ultrasonic interferometry system has been constructed in our lab as shown in Fig. 3. Now for the critical stage: alignment and testing of variety transducers. This system will allow us to determine the frequency dispersion in velocity. The frequency dispersion will allow us to discuss the relaxation related issues in this unique material. For example, based on the well-known visco-elastic theory, considering the single Debye relaxation process, the sound velocity in the viscose materials can be expressed as (Refs. 11 and 12):

$$ \upsilon^2 = \upsilon_0^2 + (\upsilon_\infty^2 - \upsilon_0^2)\frac{\omega^2\tau^2}{1+\omega^2\tau^2} . \qquad (2) $$

Where υ is velocity, υ_0 is the low frequency velocity and corresponds to the ultrasonic measurements, and υ_∞ is the high frequency limit of the velocity and corresponds to the Brillouin measurements at high pressure or lower temperature; ω is the frequency and τ is the relaxation time. When υ_0 is known, we will be able to calculate the relaxation time.

IV. Results

The photo images of 4%- and 20%-gelatin solutions as prepared are shown in Fig. 4. Before loading the solutions are refrigerated for 24 hours. Figure 5 shows the

microscopic photo images for lamb brain tissue (2 GPa) and 4%-gelatin solution (1 GPa), respectively. The samples remained transparent to visible light, and no effect of possible crystallizations were observed.

A typical set of Brillouin spectra from 20%-gelatin is shown in Figure 6. There are two pairs of peaks in each spectrum and an additional Rayleigh peak at zero frequency (elastic scattering). One pair of peaks corresponds to the longitudinal acoustic mode (L-mode), and the other pair corresponds to the transverse acoustic mode (T-mode). In addition, Fig. 7 exhibits the pressure dependence of sound velocities at room temperature. Figure 8 (a and b) shows the pressure dependence of Brillouin frequency shifts for 4%- and 10%-gelatin solutions.

V. Discussion

(1) Density calculations

The gelatin can be considered an isotropic material. We calculate the pressure dependence of density of gelatin using following equation (Ref. 2):

$$\rho - \rho_0 = \int_{P_0}^{P} \frac{\gamma}{\upsilon_L^2 - \frac{4}{3}\upsilon_T^2}\,dP, \qquad (3)$$

where ρ and ρ_0 are the density at pressure P and P_0 respectively, υ_L and υ_T are the longitudinal and transverse sound velocities respectively, and $\gamma = C_P/C_V \approx 1$ (Refs. 2, 3, and 5) is the ratio of specific heat at constant pressure and constant volume.

EOS of 20%-gelatin is fundamentally important for understanding of gelatin behavior under pressure. It provides the necessary information not only for discussing the intermolecular interaction and potential for simple fluid or solid materials, but also for

simulations or modeling of gelatin under extreme conditions. Here we analyze the *P-V* data (the pressure dependence of density) with the Vinet EOS as expressed below:

$$P = 3K_0 [\frac{1-(V/V_0)^{1/3}}{(V/V_0)^{2/3}}] \exp[\frac{3}{2}(K_0' - 1)(1-(V/V_0)^{1/3})] \qquad (4)$$

where K_0 is the bulk modulus, K_0' is its derivative at zero pressure, and V_0 is the initial volume at room temperature.

It should be noted there are two practical problems with the calculation of density. One is the assumption of $\gamma \approx 1$; the other is the accuracy of the integration of the density at lower pressure.

(A) Let us first discuss the assumption of $\gamma \approx 1$. **Heat capacity ratio**, γ, is the ratio of the heat capacity at constant pressure (C_P) to heat capacity at constant volume (C_V). It is expressed as follows:

$$\gamma = \frac{C_P}{C_V} \qquad (5).$$

In addition, the laws of thermodynamics imply the following relations between these two heat capacities:

$$C_P - C_V = VT\frac{\alpha^2}{\beta_T}, \text{ and } \frac{C_P}{C_V} = \frac{\beta_T}{\beta_S} = \frac{K_S}{K_T}, \qquad (6)$$

here $\alpha = \frac{1}{V}(\frac{\partial V}{\partial T})_P$ is the thermal expansion coefficient, $\beta_T = -\frac{1}{V}(\frac{\partial V}{\partial P})_T = \frac{1}{K_T}$ is the isothermal compressibility, $\beta_S = -\frac{1}{V}(\frac{\partial V}{\partial P})_S = \frac{1}{K_S}$ is the adiabatic compressibility, K_T

is the isothermal bulk modulus, and K_S is the adiabatic bulk modulus, respectively. Thus, it is easy to find the relationship between K_T and K_S as follow:

$$K_T - K_S = \frac{T\alpha^2}{C_P} \qquad (7)$$

One can estimate the difference between K_T and K_S if the C_P and α are known or vise versa. For example, for crystal MgO, K_T=162 GPa, and K_S=160 GPa, thus γ=1.01 (Refs. 13 and 14).

On the other hand, the heat capacity ratio (γ) for an ideal gas can be related to the degrees of freedom (f) of a molecule by:

$$\gamma = \frac{f+2}{f} \qquad (8)$$

Thus we observe that for a monatomic gas with three degrees of freedom, $\gamma = \frac{5}{3} \approx 1.67$, while for a diatomic gas with five degrees of freedom (at room temperature), $\gamma = \frac{7}{5} = 1.4$. By the way, tri-atomic gas such as CO_2 will have a γ=1.28.

Considering gelatin solutions are neither solid crystals nor gases but with the large chained -moleculars, the heat capacity ratio γ should have a value between 1 and 1.28.

(B) For gelatin solutions or polymeric materials the density changes 30 to 60% between ambient and 1 or 2 GPa, therefore the accuracy of the integration of density at lower pressure becomes very important, as shown by the following example. We plotted

the inverse of bulk sound velocity square as a function of pressure (Fig. 9a). One can calculate the density difference between points A(P1, ρ1) and B(P2, ρ2) by first calculating the shaded area between A and B, then adding them to the ρ1 to obtain the ρ2. If point B is too far from point A on the velocity curve, the density calculation will contain a huge margin of error, particularly at lower pressure where density increases drastically. To reduce the error in density calculation, we measured the pressure dependence of the sound velocity in small pressure increments as shown in Fig. 9b.

(2) 4%-, 10%-, and 20%- gelatin solutions

Figure 8 a and b shows the pressure dependencies of the Brillouin shifts of 4%- and 10%-gelatin solutions. The three-run of experiments were perfromed for 4%-gelatin at different time periods. Unfortunately, we did not obtain consistent results. We obtained similar results for 10%-gelatin solution. We suspect that the heterogenity of the sample may have played an important role in this, because our sample chamber is very small on the order of microns, about $\pi \times 60^2 \times 20$ µm^3 in size. During the loading of 4%- or 10%-gelatin samples, we could have loaded the sample that varied in concentration if compared with the originally prepared bulk sample, thereby obtaining different results for each run of experiments.

On the other hand, the results of 20%-gelatin solution displayed consistency. Figure 7 shows the pressure dependecies of the sound velocities of 20%-gelatin solution indicating consistent results for different-run of experiments. This is an important result. Furthermore, in Ref. 15 , the author separated the pressure dependence of density (data from Ref. 13) into two domains: below 2 GPa and above 2 GPa, subsequently fitting the data with Birch-Marnaghan EOS and obtaining reasonable bulk modulus for lower

pressure regime. We listed the numerical values in Table I. This assumption can be considered reasonable, because the density increased at least 30% between ambient and 2 GPa. Same trend also can be realized using Fig. 9; the inverse sound velocity square changes drastically around 2 GPa. There could exist a transition around 2 GPa as shown in Ref. 2. Thus the assumption of separating the P-V data into two domains below and above 2 GPa can be justified.

In Refs. 16 and 17, the authors considered the mechanism of light scattering from gels. They proposed that acoustic waves propagating in a gel can be divided into two groups. One is the wave propagating in the polymer network, and that other is that propagating in the fluid. Generally, these two acoustic waves couple to each other, and there is friction between the two media. Two extreme cases were considered by the authors. The first case, which predicts a two-mode type of behavior for the Brillouin spectrum, occurs for small frictional damping. In this case, two pairs of Brillouin peaks should be observed. The strong friction case predicts a single pair of Brillouin peaks. Since only one pair of the Brillouin doublets can be found in our results, it seems appropriate to consider our case are the strong friction one. Unfortunately, this theory cannot be directly applied to our case without further developing of the theory, because the interaction between polymer network and fluid is unknown under pressure.

(3) Lamb muscle and brain tissues

For comparison purposes, we also measured the pressure dependence of velocity of lamb red meat and brain tissues. All animal tissues are obtained from the open market sources (meat store or butcher shop). Figure 10 shows the Brillouin spectra from lamb brain tissue at selected pressures. It is obvious that the Brilluoin peaks are broad at very

low pressure indicating that relaxation process couples strongly to the acoustic mode. However, the discussion of the relaxation processes are beyond the scope of this report, thus we will discuss that in a separate report or paper in the near future. Figure 11 displays the pressure dependence of Brillouin shifts of L-mode for the brain tissues. Several run experiments yielded consistent results despite samples differing from each other, having been purchased at different times and definitely belonged to the different animals. It should be noted that the transverse modes are extremely weak for brain tissue, we only observed weak transverse signal for brain tissue above 4 GPa. On the other hand, the transverse modes are easy to observe from lamb red meat tissue as shown in Fig. 12. Nevertheless, all those materials behaved similarly under pressure, as shown in Fig. 13.

(4) Elastic properties

The isotropic material has two independent elastic constants: C_{11} and C_{12}. The pressure dependence of elastic constants of 20%-gelatin appear in Ref. 2. Considering we don't have knowledge about the initial density of either 4%-, 10%-gelatin or lamb tissue, it will be difficult to calculate the pressure dependence of density for them. Instead we can calculate the Poisson's ratio. The Poisson's ratio can be expressed as follows:

$$\sigma = \frac{\upsilon_L^2 - 2\upsilon_T^2}{2(\upsilon_L^2 - \upsilon_T^2)} \tag{10}$$

The pressure dependence of the Poisson's ratio for 10%-, 20%-gelatin solutions and lamb red meat tissue are shown in Fig 14. The value of Poisson's ratio is 0.36 for 20%-gelatin at 10 GPa. It is comparable with that of silicate glass at the same pressure (Ref. 16). The Poisson's ratio of a stable, isotropic, elastic material cannot be less than -1 nor greater than 0.5 due to the values of Young's modulus, shear modulus, and bulk modulus

required to be positive. Most materials have a value between 0 and 0.5. A perfect incompressible material such as rubber, when deformed elastically under small strain would have a value of 0.5 for its Poisson's ratio. Most metals have a value around 0.35. For gelatin solutions, particularly at lower pressures, we did not obtain the transverse sound velocities, thus we cannot use Eq. (10) to calculate the Poisson's ratio for that pressure regime.

In addition, we obtained measurements of the Poisson's ratio at lower pressure regime (Fig. 14). One can speculate that in addition to the error due to the weak intensity of the transverse mode at lower pressure regime, the absolute pressure error is about 0.2 GPa; thus it has larger relative errors at lower compared to higher pressures. These relative errors convelote to the uncertainty in the velocity measurement. Because the Poisson's ratio is close to the ratio of the velocity squared, the errors would be amplified. Inspection of Fig. 14 shows that the Poisson's ratio for gelatin and lamb tissue increase with pressure up to 2 GPa, indicating materials are more compressible at lower pressure as expected.

We also compared the bulk modulus and its pressure derivative with several polymers and water. We listed all relevant numbers in Table I. It should be noted that bulk modulus for these materials tend to have a smaller value, indicating these materials are easy to compress. On the other hand, the values of the pressure derivative of these materials vary largely and depend on the material. For crystal-like materials including minerals, in most cases, the pressure derivative of the bulk modulus varies around 4 (Refs. 13 and 14).

VI. Conclusion

We determined the equation of state for ballistic gelatin using a combination of Brillouin scattering and diamond anvil cell techniques. We measured the sound velocities of 20%-, 10%-, and 4%- gelatin solutions between ambient and 12 GPa. In addition, we measured the pressure dependence of the sound velocity of Lamb tissues for comparison purposes. We analyzed the Brillouin data using the Vinet equation of state and obtained the bulk modulus, its pressure derivative. We also compared the gelatin bulk modulus and its pressure derivative with several relevant polymer materials as well as water.

Acknowledgments

VII. References:

1. http://www.vyse.com/gelatin_for_ballitic_testing.htm.

2. M. Aihaiti, R. J. Hemley, *Equation of State of Ballistic Gelatin*; 50533-EG.1; Carnegie Institution of Washington, 2008. http://handle.dtic.mil/100.2/ADA501428.

3. C. S. Zha, et al, Phys. Rev. B **50** 13105 (1994).

4. M. Ahart, A. Asthagiri, Z. G. Ye, P. Dera, H. K. Mao, R. E. Cohen and R. J. Hemley, Phys. Rev. B **75**, 144410 (2007).

5. M. Ahart, J. L. Yarger, K. M. Lantzky, S. Nakano, H. K. Mao and R. J. Hemley, *J. Chem. Phys.* **124**, 14502 (2006).

6. Sandercock, J. R., *Trends in Brillouin-Scattering - Studies of Opaque Materials*, Supported Films, and Central Modes, in *Light Scattering in Solids III. Recent Results* (eds. M. Cardona and G. Guntherodt) Berlin, Springer -Verlag., **51**, 173 (1982).

7. K. Matsuishi, et al, J. Phys.: Condens. Matter **14**, 10631 (2002).

8. K. Matsuishi, E. Gregoryanz, H. –K. Mao, R. J. Hemley, J. Chem. Phys. **118**, 10683 (2003).

9. W. A. Bassett, H. –J. Reichmann, R. J. Angel, H. Spetzler, and J. R. Smyth, Amer. Miner. 85, 283 (2000).

10. H. –J. Reichmann, R. J. Angel, H. Spetzler, and W. A. Bassett, Amer. Miner. 83, 1357 (1998).

11. Y. Takagi, M. Ahart, T. Yano, S. Kojima, J. Phys.: Condens. Matter 9, 6995 (1997).

12. W. F. Oliver, C. A. Herbst, S. Lindsay, G. H. Wolf, Phys. Rev. Lett. **67**, 2795 (1991).

13. R. J. Angel, Rev. in Mineral. Geochem. **41**, Mineral Soc. Of Am., Washington DC, P35, eds. R. Hazen, and R. Downs.

14. S. H. Shin, and T. S. Duffy, J. Geophys. Res. **105**, 25955 (2000).

15 Y. Huang, *Gelatin Equation of State Characterization Progress;* Army Research Laboratory, ARL-MR-0727, 2009.

16. J. A. Marqusee and J. M. Deutch, J. Chem. Phys. 76, 5239 (1981).

17. P. Zhao and J. J. Vanderwal, Polymer Gels and Networks 5, 23 (1997).

18. L. L. Stevens, E. B. Orler, and D. M. Dattelbaum, M. Ahart and R. J. Hemley, J. Chem. Phys. 127, 104906 (2007).

19. L. L. Stevens, E. B. Orler, and D. M. Dattelbaum, M. Ahart and R. J. Hemley, Materials Lett. Submitted.

20. J. M. Brown, L. J. Slutsky, K. A. Nelson, L. T. Cheng, Science **241**, 65 (1988).

21. A. Polin, M. Grimsditch, Phys. Rev. B 27, 6407 (1983).

22. M. Ahart, M. Somayazulu, S. A. Gramsch, R. Boehler, H-k. Mao, R. J. Hemley, J. Chem. Phys., accepted.

Table I: bulk modulus comparison for several polymers and water-ice

materials	Bulk modulus (GPa)	pressure derivative	references
20%-gelatin	4.9	8.2	This work
20%-gelatin	1.52	13.88	Ref. 13 (Vinet EOS)
20%-gelatin	0.94	34	Ref. 13 (Brich-Marnaghan EOS)
VCE polymer	2.05	9.99	Ref. 18
Estana	2.84	17.1	Ref. 18
Sygard	1.13	8.95	Ref. 18
Kel-F800	7.5	10	Ref. 19
n-pentane/ isopentane	0.45	10.5	Ref. 12
Methanol	0.96		Ref. 20
Water	2.4		Ref. 21
Ice VII	5	8.1	Ref. 22
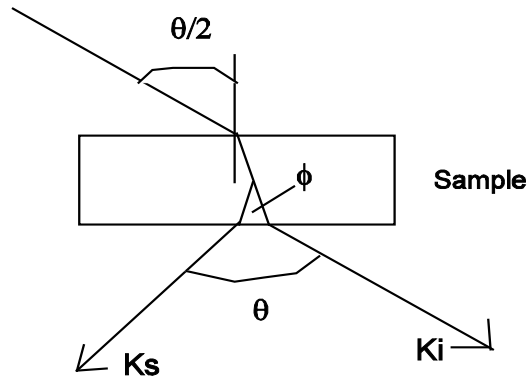
Figure 1. Schematicdiagram of the symmetric scattering geometry. The incident light enters the sample with the angle $\theta/2$, and by Snell's law the following equation will hold: $n_0\sin(\theta/2)=n\sin(\varphi/2)$, where n_0 is the refractive index of air and n is the refractive index of samples. Therefore the Brillouin shifts will have the following form: $\Delta v_\varphi = \dfrac{2nv}{\lambda}\sin(\varphi/2) = \dfrac{2v}{\lambda}\sin(\theta/2) = \Delta v_\theta$. The Brillouin shifts are defined uniquely by the scattering angle between incident and scattering light.
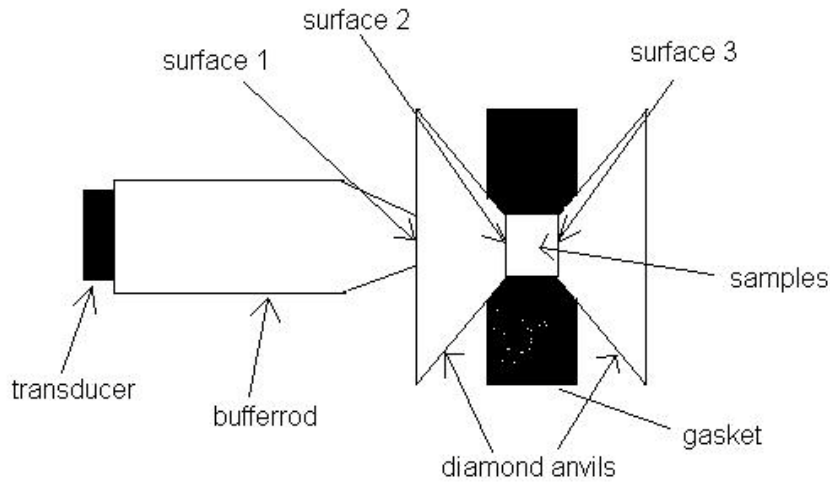
(a)
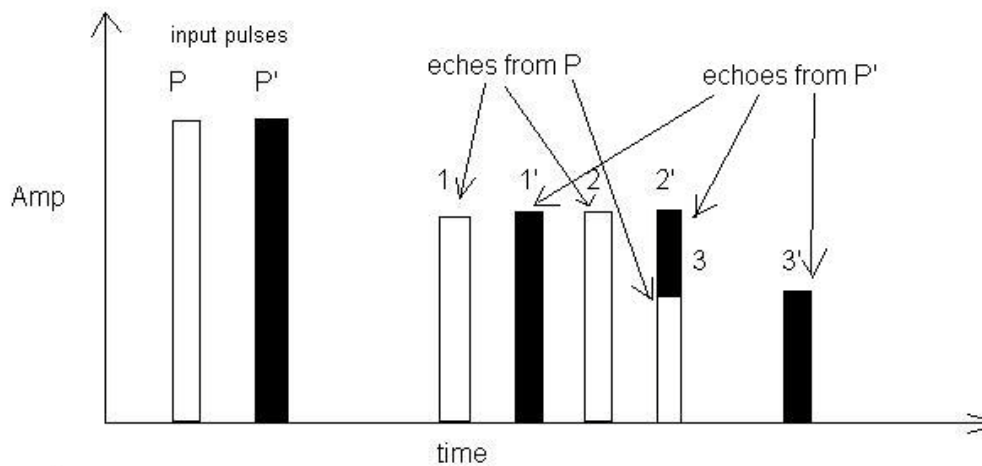
(b)

Figure 2. Two closely spaced pulses (P and P') can be carefully timed so that the reflection of the first pulse from the far surface of the sample (echo 3) is superimposed on the reflection of the second pulse from the near surface of the sample (echo 2'). Travel time of the signal through the sample can be calculated from the interference between these two signals as they return to the transducer. This simple diagram is adapted from Ref. 9.
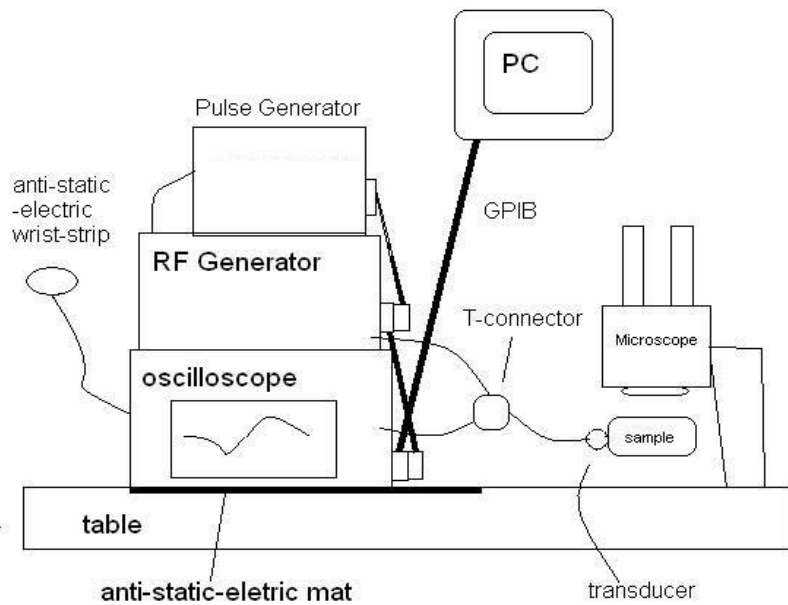
Figure 3. A schematic diagram for our ultrasonic interferometry system. A pulse signal generated from signal generator is sent to transducer. The transducer contacts the diamond anvil cell and samples as in Fig.2. The fast sampling oscilloscope will collect the signal from samples' two surface and compare them to the incident pulse.
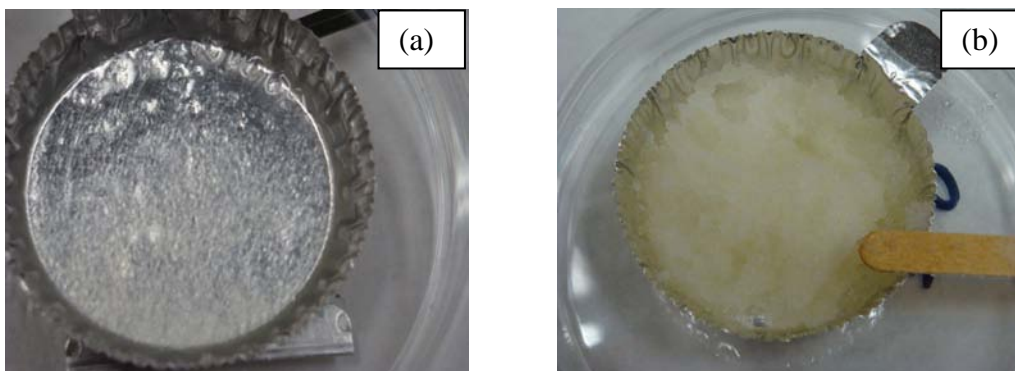
Figure 4. The photo images of gelatin solutions as they were taken after the gelatin powders were mixed with water; (a) 4%-gelatin solution; (b) 20%-gelatin solution. Before loading, gelatin solutions were refrigerated for at least 24 hours.
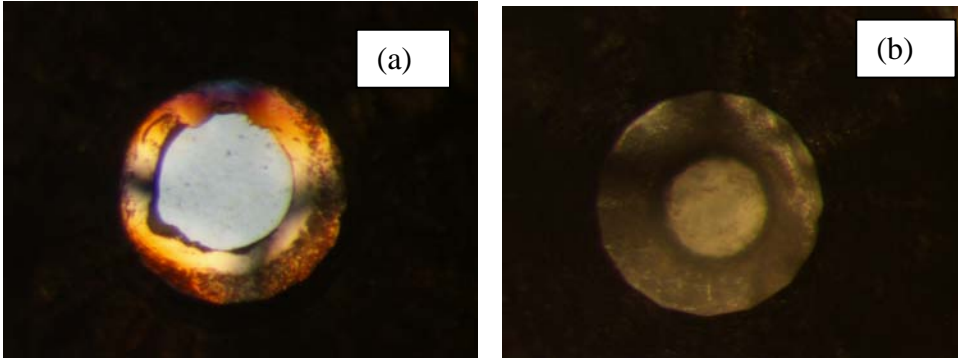
Figure 5. The microscopic photo images of gelatin solutions and lamb brain tissue in a diamond anvil cell; (a) lamb brain tissue at 2 GPa (used brighter light); (b) 4%-gelatin solution at 1 GPa (used dimmer light).
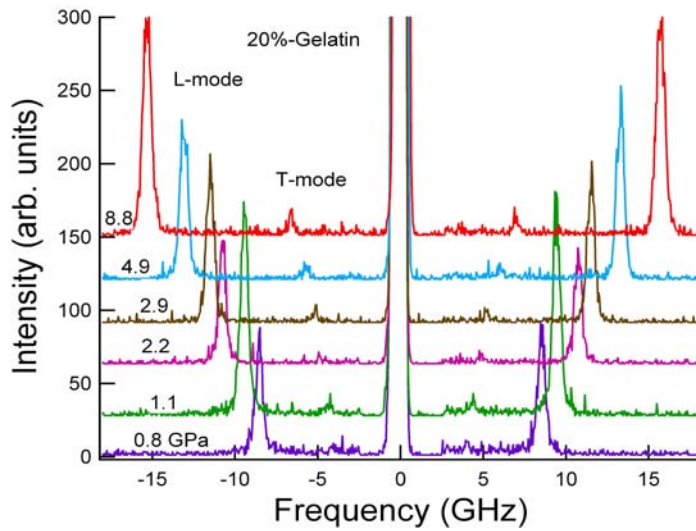
Figure 6. A set of typical Brillouin spectra of 20%-gelatin. The elastic scattering line at the zero frequency. The Brillouin lines at around 4 and 8 GHz for transverse and longitudinal acoustic mode at 0.8 GPa, respectively.
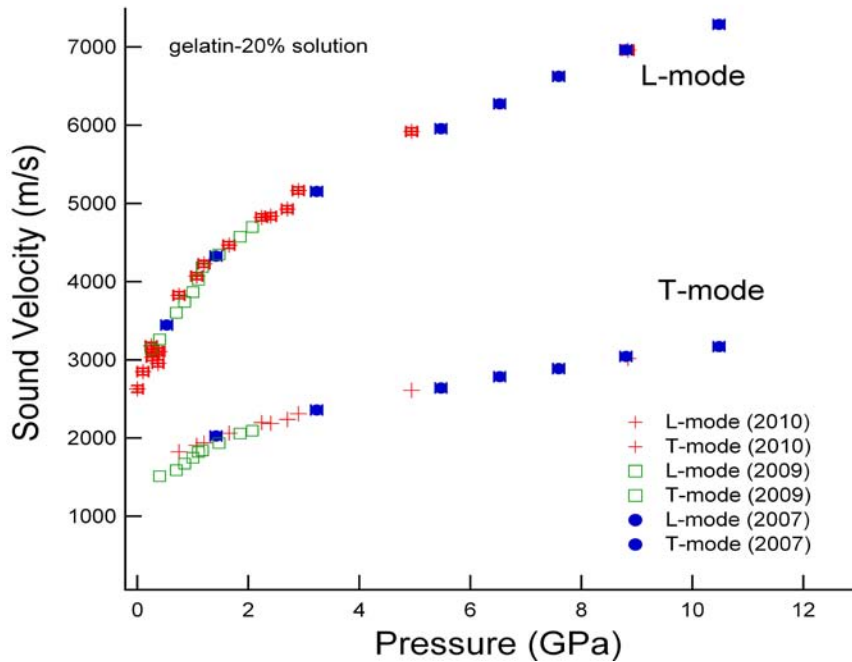
Figure 7. Pressure dependencies of sound velocities of 20% gelatin solution. To confirm the reproducibility, we did measurements using separately prepared samples at different time periods. Different symbols represent different measurements. The error bars are given in the figure. They are similar to the size of the symbols.
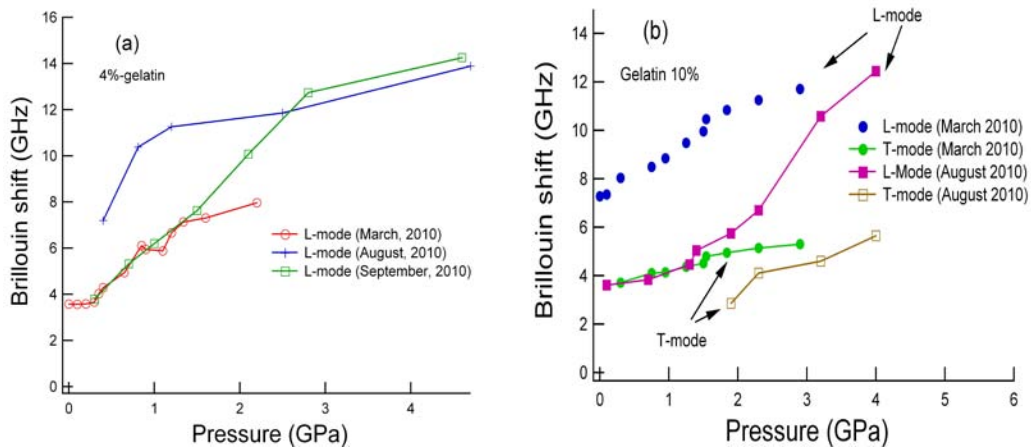
Figure 8. Pressure dependencies of the Brillouin shifts of 4%- and 10%-gelatin. (a) The three-run of experiments were performed for 4%-gelatin at different time periods; (b) two-run of experiments were performed for 10%-gelatin. We did not obtain consistent results.

22
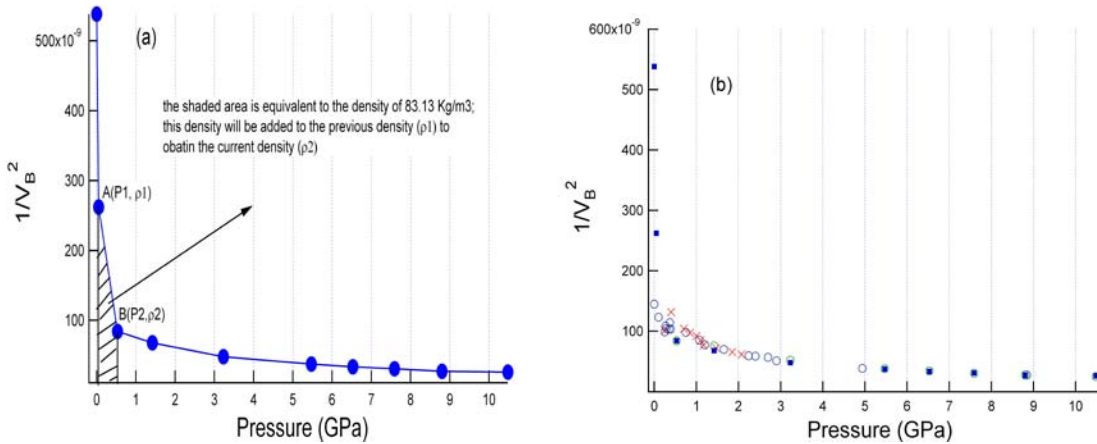
Figure 9. Pressure dependence of the inverse velocity square. (a) This diagram explains how we calculate the density for each pressure point; (b) particularly at lower pressure regime, more data points are needed in order to obtain more accurate density.
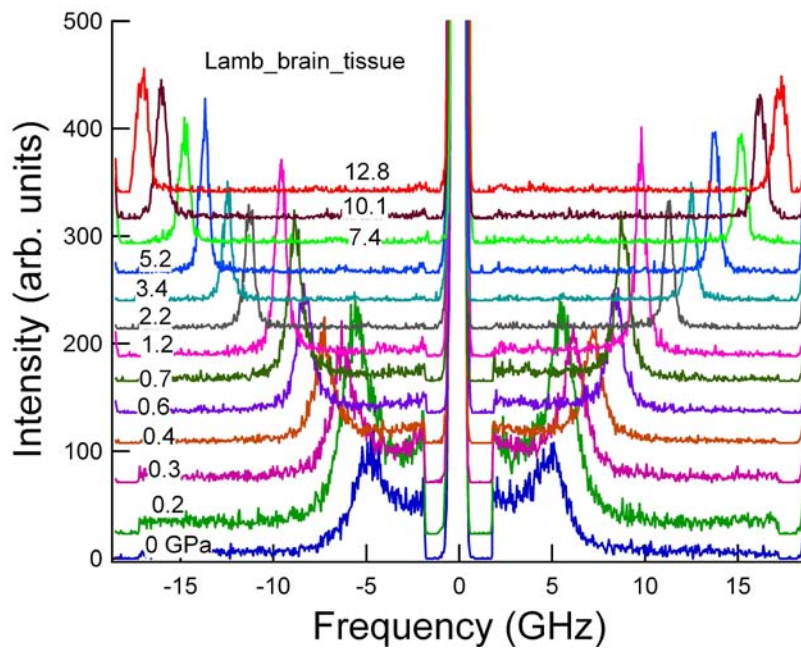

Figure 10. A set of Brillouin spectra of lamb brain tissue at selected pressures. The transverse mode is weak and difficult to read directly from spectra. Each spectrum must be enlarged in order to read the transverse mode.
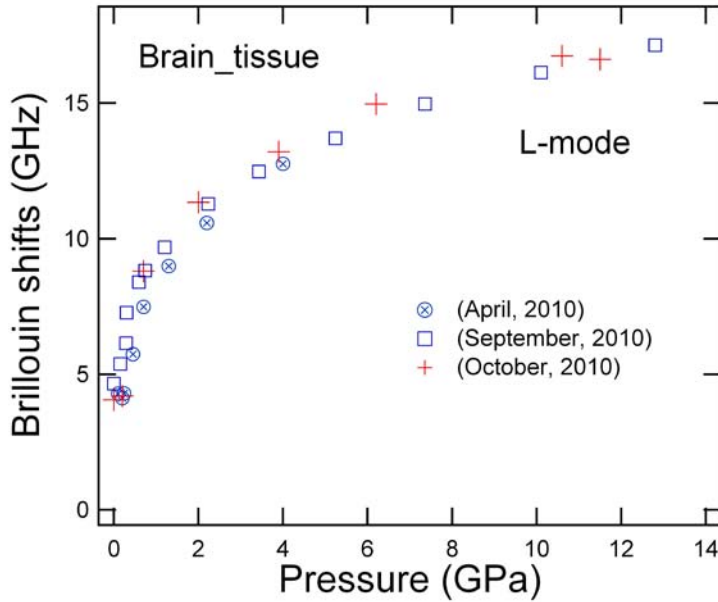
Figure 11. Pressure dependence of longitudinal mode (Brillouin shifts) of lamb brain tissue. Relatively, brain tissues show consistent results if compared with the 4% or 10%-gelatin solutions.
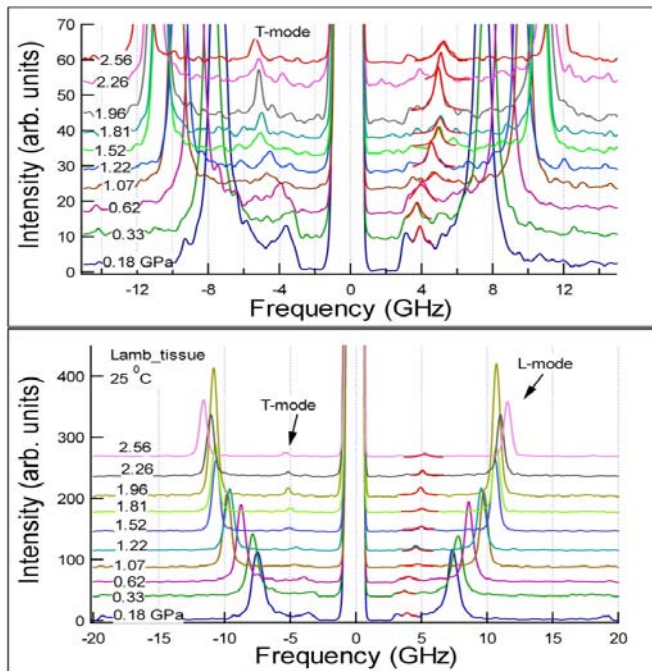

Figure 12. A set of typical Brillouin spectra of lamb red meat tissue at selected pressures. The transverse modes (T-mode) are obvious in the spectrum. To emphasis the transverse mode the upper frame of the figure enlarged the spectra.
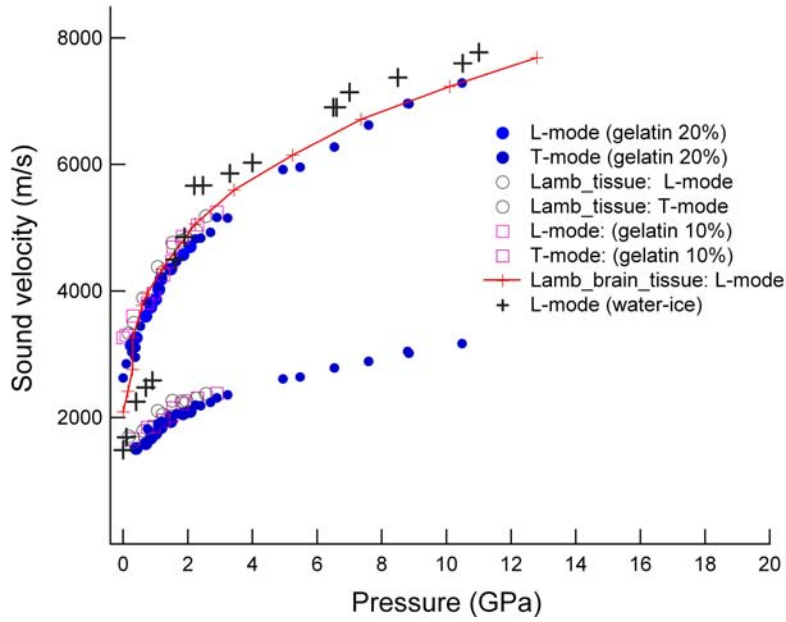
Figure 13. Pressure dependencies of the sound velocities of gelatin solutions, Lamb tissues, and water-ice. Solid circles correspond to the longitudinal and transverse acoustic mode of 20%-gelatin; open circles represent the acoustic modes from the lamb red meat tissue; open squares are the marks for 10%-gelatin samples; solid curve with cross marks correspond to the longitudinal mode of the lamb brain tissue, respectively.
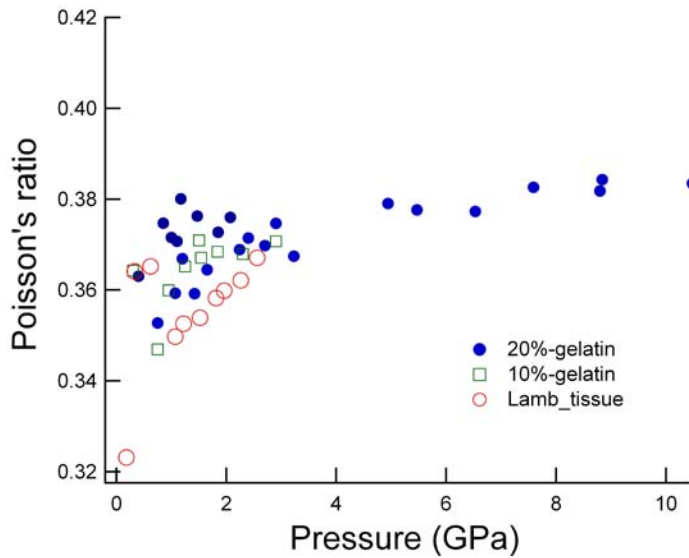

Figure 14. Pressure dependences of the Poisson's ratio at room temperature.